Self-regulation of a network of Kuramoto oscillators

Author: Paula Pirker Díaz*
Màster en Física dels Sistemes Complexos i Biofísica.
Facultat de Física, Universitat de Barcelona, Martí i Franquès 1, 08028 Barcelona, Spain.†

Advisors: Dr Albert Díaz-Guilera and Dr Jordi Soriano Fradera
Facultat de Física, Universitat de Barcelona, Martí i Franquès 1, 08028 Barcelona, Spain.
(Dated: May 20, 2023)

Abstract: Persistent global synchronization of a neuronal network is considered a pathological, undesired state. Such as synchronization is often caused by the loss of neurons that regulate network dynamics, or cells that assist these neurons such as glial cells. Here we propose a self-regulation model in the framework of complex networks in which we assume that, for sake of simplicity, glial cells prevent the over synchronization of the neuronal network. We have considered a brain-like network characterized by a modular organization combined with a dynamic description of the nodes as Kuramoto oscillators. We have applied a self-regulation mechanism to keep local synchronization while avoiding global synchronization at the same time. To do so, we have added self-regulation to the system by switching off for a certain period of time a selection of edges that link nodes showing a synchronization above a certain threshold. Despite the simplicity of the approximation, our results show that it is possible to maintain a high local synchronization (module level) while keeping low the global one. In addition, characteristic dynamic patterns have been observed when analysing synchronization between modules in large modular networks. Our work could help to understand the effects of localized regulatory actions on modular systems with synchronous phenomena, such as neuroscience and other fields.

I. INTRODUCTION

Synchronization can be found in multiple phenomena in nature. The synchronous flashing of fireflies, the cardiac pacemaker cells or the synchronized clapping of a crowd are just some examples. [1, 2] One of the fields where synchronization plays a crucial role is neuroscience. There is a broad experimental evidence of neuronal oscillatory activity, which has been related to cognitive activities such as memory, learning, and perception [3].

Neuronal synchronization phenomena are taken into account in general for a deeper understanding about information processing, as well as in determining normal and abnormal brain function. Indeed, neurological diseases as epilepsy, Parkinson's, Alzheimer's, autism or schizophrenia, have been often related to alterations in neuronal synchrony [2–4]. Concretely, many of these pathologies are related to an excessive level of global synchronization and there is experimental evidence that global synchronization is not present in well-functioning brains [2, 5], which actually switch between global and local states. In this direction, many studies have highlighted the role of local synchronization in a wide variety of processes, specially in memory processes [6], perception, or visual recognition system [7]. Due to the important implications of synchronization, the understanding of this phenomena is relevant to the field of neuroscience. It is well accepted that there are desirable levels of synchronization, but the way a healthy brain switches between them is not fully understood.

The nervous system is formed by two main cell types, neurons and glial cells, which are divided in turn into several subgroups with different functions, from excitatory and inhibitory neurons to, for the case of glia, oligodendroglia, microglia, ependimoglia and astroglia [8]. While neurons are considered as the main computational units involved in the transfer and processing of information, glial cells play a crucial role in maintaining neurons, and the connections they form, in perfect condition. Particularly astrocytes, the most abundant glia type in the nervous system, are known for their involvement in metabolic support, neuronal survival and differentiation, synapse formation, regulation of the local concentrations of ions and neurotransmitters, as well as the control of local cerebral blood flow [8, 9].

As a consequence, it is logical to think that brain functions result from the collective activity of neurons and glial cells and that both must be taken into account to understand it. In reference to synchronization, it is known that glial cells, mainly astrocytes and oligodendrocytes, influence processes underlying local neuronal oscillations, like neuronal membrane potential and synaptic transmission [8]. There are studies that suggest that a reduction in astrocytic coupling may cause hyperexcitability and, consequently, lead to synchronization of neuronal activity [10]. Thus, glial cells contribute to the regulation of network activity and, hence, help tuning the synchrony state of the system. Sometimes this contribution is indirect, which illustrates the complexity of biological neuronal networks. For instance, in some genetic variants of Parkinson's disease, the degradation and loss of glia cells cause the death of dopaminergic neurons, fundamental in regulating network activity, leading to a persistent,

* ppirkedi7@alumnes.ub.edu
† master.complex.biophys@ub.edu

uncontrollable global synchronization [11].

All the above considerations shape the biological inspiration and starting point of this project, namely that glial cells are —directly or indirectly— the regulatory agents of their surrounding neurons that keep synchronization in a desired level.

We tackled the problem using numerical simulations. Indeed, *in silico* modelling is a powerful tool and has become an active research area in neuroscience. It combines physical and mathematical tools to simulate and analyse certain situations, as well as to study the effects of different parameters in a completely controlled environment. Synchronization in networks of oscillators have been widely studied [1], but the development of methods in order to control the behavior of the emerging dynamical system has only recently awakened interest [12–15]. Some of these studies focus on the structure a network should have in order to reach a certain synchronization behaviour [13], while others focus on adjusting oscillator coupling strengths [12] or the interconnection weights [14] to promote the stability of certain functional patterns. However, in this project we propose another approach based on the control of differentiated global and local synchronization.

Thus, in this work, we consider an interwoven network of glial cells and neurons, and assume that the glia cells regulate the synchronization of the neuronal network they nurse. For that, we consider a network of Kuramoto oscillators and propose a simple self-regulation model to control the level of global and local synchronization. Conceptually, we model a 'toy brain' in which each oscillator represents a large population of neurons. The oscillators, for sufficiently strong coupling, will tend to spontaneously synchronize in a global manner. To prevent that, we act locally (through the presence of glia) by switching on or off a set of edges.

To define our problem, we firstly set up the assemble of oscillators as a modular network, where each module is constructed as a random geometric graph. There are several studies that consider small-world networks or other network structures without metrics [3], meaning that the distance between nodes (i.e., the Kuramoto oscillators) is completely irrelevant. Nevertheless, real neuronal networks are embedded in a bi-dimensional space and it is well known that near neurons or brain areas are more likely to be connected than remote ones [16, 17]. Therefore, taking into consideration the importance of spatial constraints, here we generate each module of the network as a random geometric graph, which considers that connectivity is more favorable at short Euclidean distances. At the end of the construction, all modules are connected to the neighbouring ones to form the modular network. It must be noted that modular is an ubiquitous trait of neuronal networks, and it has been seen at different scales in the brain, from neuronal communities to brain regions [18]. It is remarkable to say that we compare the response to the proposed model of two different network structures defining the system. Both of them modular, but with a different size though having similar network properties.

Secondly, we make the network of oscillators tend towards synchronization. There are several models that lead to that behaviour and here we opt for the Kuramoto model, which is one of the simple models for describing phase dynamics in multiple fields, including neuroscience. Then, we apply a simple self-regulation process in order to keep local synchronization while avoiding a globally synchronous state. The self-regulation process consists in the control and deletion of edges connecting too much synchronized nodes and this control is performed exclusively over edges within certain regions representing the domain of the regulatory agents, i.e. our idealized glial cells. Once an edge is being deleted we add the possibility of recovering it after a certain period of time, making the system more interesting, for instance to capture the concept of healing after damage.

We must note that our system is a highly simplified model of a biological neuronal network. However, the obtained results are certainly interesting. The results show that global synchronization can be remarkably reduced while keeping local synchronization stable and high. Moreover, we have seen that the network has to be non-random for interesting phenomena to emerge. In addition, we have analysed the effects of modularity and the interaction among modules during the dynamic evolution of the network, observing that interesting patterns of interaction among modules emerge and are maintained.

The present work is organized as follows. We first introduce the network generation method that will be used henceforward. Next, we present the model by introducing the Kuramoto model and the proposed self-regulation process. All results are shown in the next section and the discussion and conclusions are provided together with some perspectives at the final part.

II. NETWORK GENERATION

To study the proposed self-regulatory dynamics, we start with a simple representation of a neuronal network as a set of nodes with dependencies characterized by undirected and unweighted edges between them. In this scenario, the system is defined by an *in silico* neuronal network formed by nodes representing groups of neurons idealized as oscillators, and edges that may be thought as the synaptic connections among them. The networks generated are formed by M interconnected modules created as random geometric graphs of equal number of neurons, N. The followed steps are the next ones:

1. Creation of M random geometric graphs. To do so, N nodes are randomly set on a two-dimensional squared surface, $L \times L$, and each one of them is connected to any other one located in a distance smaller than a neighbourhood radius ρ with probability γ. The latter process is repeated M times.

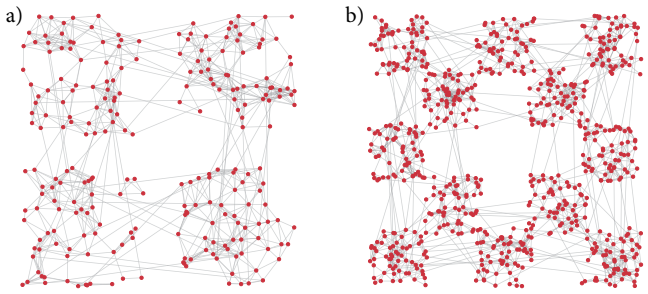

FIG. 1. Graphs of the two types of simulated networks. *a*) Network of 4 random geometric modules of $N = 60$ nodes each, generated defining (L, ρ, γ, n_c)=(25, 6, 0.8, 24). It is worth mentioning that as each module is connected to only two of the others, the 24 inter-modular edges are equally distributed between them. *b*) Network of 12 random geometric modules generated with the same parameters as the previous case. However, each module is connected to its neighbouring ones by a total number of 24 edges not equally distributed among the neighbours so as to keep n_c= 24 to all modules.

2. Connection of the M random geometric graphs. The M graphs of the previous step are connected in order to obtain the final modular network. For this purpose, the M graphs are distributed as desired in the plane keeping the relative positions of all nodes of every single graph. Then, n_c connections are established between modules just by linking randomly selected nodes from the modules we are interested in. For example, if modules 1 and 2 are wanted to be connected by i edges, i links connecting randomly selected nodes are added from module 1 to module 2. Since real neuronal cultures are spatial networks, each module is connected only to the neighbouring ones and n_c is considered to be the sum of all the inter-modular edges of each module.

In this work we have analysed two different network structures: one with 4 modules, forming what is known as ring modular network, a quite common structure in *in vitro* experiments [19]; and another one with 12 modules so as to analyse the effect of network's topology on the dynamics proposed. Both types share the same parameters when creating the random geometric graphs forming the modules, but differ in the number of modules and their spatial distribution. Representative graphs of the mentioned network types can be found in Fig. 1 and the average structural properties over 100 realizations of both types are presented in Table I.

TABLE I. Averaged structural properties of the two network types analysed taking 100 networks of each.

	$n = 4$	$n = 12$
Nodes	240	720
Edges	1040.90	3108.16
Average degree	8.67	8.63
Diameter	8.80	12.58
Clustering	0.58	0.57
Modularity	0.73	0.78

III. THE MODEL

The dynamics of a network of synaptically interacting neurons can be approximated by a network of phase oscillators. We can model each neuron as a phase oscillator producing an action potential when its phase equals 0 or 2π, as suggested in [12, 20, 21].

There are many oscillators models and one of them is the Kuramoto model, which makes possible the analysis of periodic dynamics of elements interacting continuously in time. The strong points motivating the choice of the Kuramoto model have been its widespread use, derived from its simple and intuitive construction, together with its rich dynamical repertoire. In the next sections we discuss the Kuramoto dynamics and the purposed dynamics, which consists in the addition of self-regulation.

A. Kuramoto dynamics

The Kuramoto model was proposed by Y. Kuramoto in 1975 [22] and describes the dynamics of a system of oscillators where each oscillator continuously redefines its effective frequency to minimize the difference between its own phase and the phase of its neighbours. Although every oscillator has an intrinsic frequency, they influence one another pulling on their frequencies. As a consequence, the instantaneous frequency of each oscillator is defined by its intrinsic frequency and by the influence of its neighbours.

Considering a group of N coupled oscillators (i.e. neurons) with phase $\theta_i(t)$ and with natural frequencies ω_i (i.e. spiking rates) distributed with a given probability density $g(\omega)$, the Kuramoto model reads:

$$\dot{\theta_i} = \omega_i + K \sum_{j=1}^{N} A_{ij} \sin(\theta_j - \theta_i), \tag{1}$$

where K is the coupling interaction strength (i.e. representing our synaptic weight) and A_{ij} corresponds to the adjacency matrix defining the interactions (connectivity) of the system.

On the one hand, the natural frequency term makes each oscillator run independently of the others. On the other hand, the coupling term that depends on the sine of the phase difference makes each oscillator readjust its

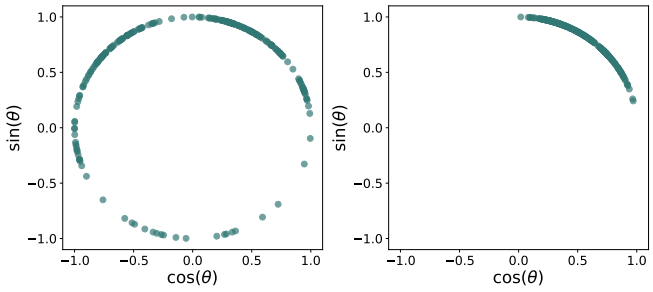

FIG. 2. Phases of a system of Kuramoto oscillators for two different time steps of the same realization. Left: very poor correlation between phases. Right: strong correlation; after some time steps, the system ends up showing a very similar phases.

phase to synchronize it to the others. Therefore we have two different trends and synchronization can be reached depending on the strength of the coupling.

If the coupling K is weak with respect to the variance of the frequency distribution, oscillators do not reach synchronization (relationship showed in the following paragraphs). However, if the coupling is strong enough, the system ends up reaching a synchronous state in which effective frequencies and phases tend to be similar despite having started with a random distribution of initial phases (Fig. 2). Hence, the values of K and $g(\omega)$ turn out to be crucial for the evolution of the system.

As we are interested in the collective behaviour, we define the order parameter $r(t)$ capturing the similarity between phases as:

$$r(t)e^{i\Psi(t)} = \frac{1}{N}\sum_{j=1}^{N} e^{i\theta_j(t)}, \tag{2}$$

where $\Psi(t)$ corresponds to the mean phase of the system and $0 \leq r(t) \leq 1$ can be understood as a measure of the degree of synchronicity, being $r(t) = 0$ for the case of a completely incoherent state and $r(t) = 1$ the case for an absolutely coherent one.

As shown in Fig. 3, if we let a system with an initial state formed by randomly distributed phases evolve following the Kuramoto dynamics, an increase of $r(t)$ is expected with an steepness that will depend on the value of K. For large values of K, synchronization is easier to reach and that can be appreciated with a faster approach of $r(t)$ to 1.

Regarding the evolution of K, two different phase transitions can be appreciated. On the one hand, we can see a transition in time from disorder to order that gets much steeper at large values of K (see Fig. 3a). On the other hand, if we keep the stationary value of the order parameter for different values of K, we can appreciate a kind of second-order transition from states that do not reach synchronization to states that end up reaching it when the coupling strength, K, is increased (see Fig. 3b). Up until about $K = 0.005$ the system remains unsynchronized,

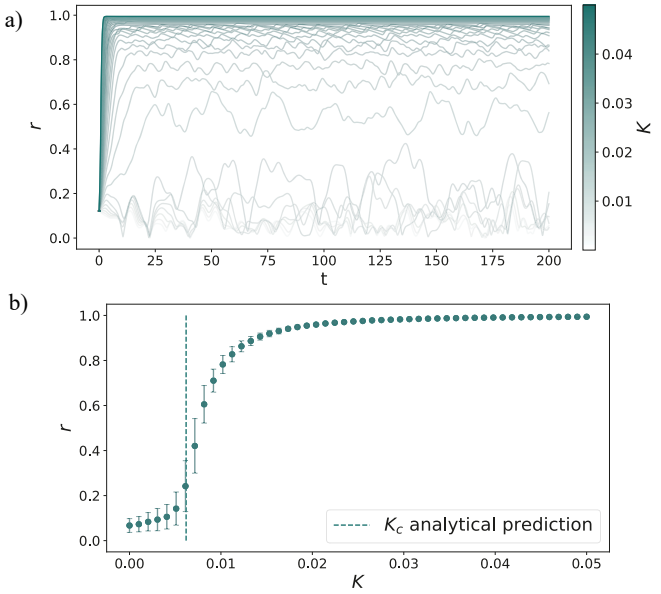

FIG. 3. *a)* Time evolution of the order parameter $r(t)$ for different coupling strength, K, values. These results com from a system of Kuramoto oscillators with a network of interaction formed by a random geometric graph with parameters (N, L, ρ)=(200, 50,10). *b)* Plot of the mean value of the time-averaged order parameter in the saturation region for different values of the coupling strength K. The mean values has been computed taking 100 realizations for each case, the error bars correspond to the variance and the plot includes the analytical prediction of the critical value of the coupling strength, $K_c = 0.00619$.

but for higher values of K the final order parameter starts rising from zero up towards one. It is worth mentioning that the final degree of synchronization reached by the system does not depend on the initial state.

This behaviour leads to the existence of a critical coupling strength, K_c, and it can be analytically predicted through the mean field result

$$K_c = \frac{2\langle k\rangle}{\pi g(\Omega)\langle k^2\rangle}, \tag{3}$$

where Ω is the center of symmetry of the distribution of natural frequencies, $g(\omega)$; $\langle k\rangle$ the average degree and $\langle k^2\rangle$ the average squared degree of the network representing the system [23, 24].

If we consider $g(\omega)$ to be a Gaussian distribution with standard deviation σ and mean $\mu = \Omega$, Eq. (3) can be rewritten as

$$K_c = \frac{2\langle k\rangle}{\pi\frac{1}{\sqrt{2\pi\sigma}}\langle k^2\rangle} = \sqrt{\frac{8}{\pi}}\sigma\frac{\langle k\rangle}{\langle k^2\rangle}. \tag{4}$$

The possibility of getting the critical prediction of the coupling strength, K_c, is really useful, as it allows us to predict beforehand if the system will end up in synchrony or not by knowing the values of σ, $\langle k\rangle$ and $\langle k^2\rangle$.

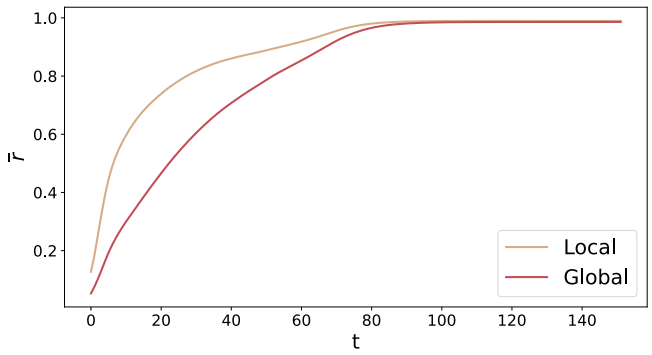

FIG. 4. Mean time evolution of both global and local order parameters over 10 simulated realizations taking the 4 modules network, the initial phases uniformly distributed between $-\pi$ and π, $g(\omega)$ as $\mathcal{N}(1,1)$ and defining $K = 2$.

At this point it is interesting to consider the dynamic behavior of the modular networks presented in the previous section.

1. *Effect of modularity*

Modularity provides richer results when applying the Kuramoto dynamics. Modular networks firstly exhibit collective synchronized patterns within each module, and later on, all modules get synchronized, leading to a local synchronization of the system followed by a global one. In other words, two different time scales can be appreciated, one for each module and another one for the whole network.

In order to quantify the level of global synchronization, we have used the aforementioned order parameter, Eq. (2). However, for quantifying the level of local sync we have to define another order parameter, which is computed as the mean value of the order parameter resulting from each module, I, over the total number of modules of the network, M:

$$r_I(t)e^{i\Psi_I(t)} = \sum_{j\in I} e^{i\theta_j(t)}, \tag{5}$$

$$r_{local}(t) = \frac{1}{M}\sum_{I=1}^{M} r_I(t). \tag{6}$$

If we let the ring modular network to follow the Kuramoto dynamics and we compute the local and global order parameters as mentioned, we can see that the local order parameter grows faster than the global one, although both reach $r = 1$, meaning that global and local synchronization are reached but at a different pace, as already expected (see Fig. 4).

In the next sections we refer to the global order parameter $r(t)$ as $r_{global}(t)$, and we take $r_{local}(t)$ as the local order parameter as already mentioned.

B. Application of self-regulation

To provide a simplified model of the regulatory properties of glial cells, we assume that they have an influence on their neighbourhood. For this reason, bearing in mind this localized behaviour, self-regulation has been proposed as the definition of regions —that we will refer to as switchers—, where all edges intersecting them are regulated. These switchers can be interpreted as the action domain of the regulatory agents of the system, i.e. the glial cells.

The proposed regulation consists in the possible deletion of the edges connecting nodes with phases θ_i and θ_j, giving a value of $\cos(\theta_i - \theta_j)$ above a certain synchronization threshold, σ_{th}. By doing so, only edges connecting highly synchronized nodes can be deleted in order to avoid global synchronization. At the same time, we have also considered the option of recovering previously deleted edges with a probability, p_r.

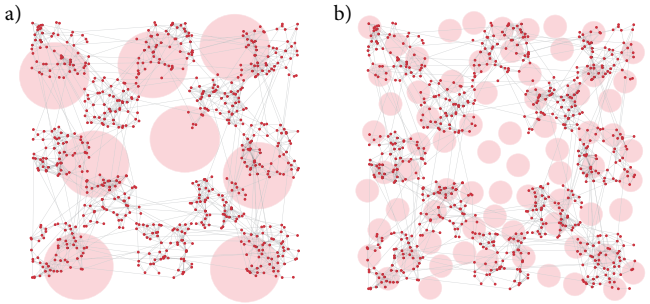

FIG. 5. Representation of the same network of 12 modules including the switchers representing the domain controlled by glial cells in pale red. *a*) Switchers defined by 8 circles of radius $R = 15$. *b*) Switchers defined by 72 circles of radius $R = 5$. It is important to mention that both cases have exactly the same surface covered by the switchers.

To explore the emerging dynamics, we first need to define the location and area of action of the mentioned switchers. Thus, the switchers are defined as circular regions of radius R randomly distributed on the plane containing the network (see Fig. 5). However, it must be noted that not only the number of switchers matters, but also the area covered by each one, since it will ultimately set its regulation role. Indeed, a larger number of small switchers intersect with a greater number of edges than a smaller number of larger switchers despite keeping the surface coverage constant, as can be seen in Fig. 6.

This result evinces that small sized switchers are much more efficient than fewer but larger ones, a trait that is merely due to geometry. Interestingly, from a biological point of view, one could say that it is worth spending more energy in order to have more but smaller-sized regulatory agents.

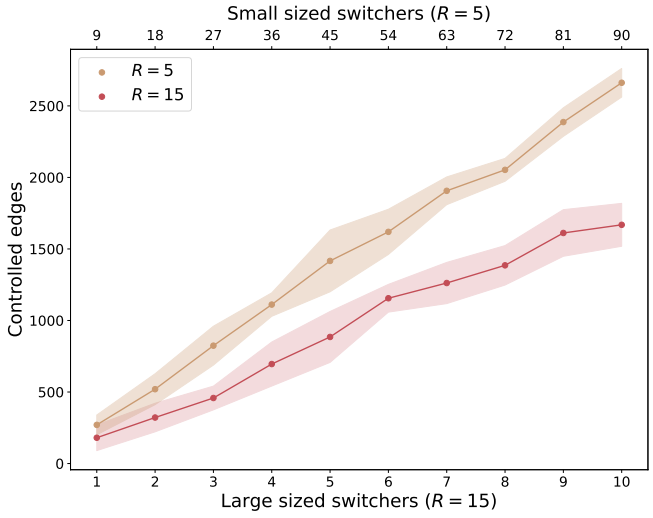

FIG. 6. Average number of controlled edges in terms of the number of switchers represented by circles of radius $R = 5$ (upper axis) or $R = 15$ (lower axis) randomly distributed as shown in Fig. 5. The average has been done over 10 realizations, each one consisting in the generation of a network of $n = 12$ modules with the same parameters as the one shown in Fig. 1b and a random distribution of the switchers for each case. It is noteworthy that vertically aligned data points correspond to the same surface covered by the corresponding switchers.

Once the network and the switchers are defined, the presented dynamics consists in the next steps:

1. Definition of the dynamic parameters: coupling strength, K; synchronization threshold, σ_{th}; and recover probability, p_r.
2. Definition of the initial conditions of the system: natural frequencies, ω_i, distributed with a given probability density $g(\omega)$; initial phases, θ_i, uniformly distributed between $-\pi$ and π.
3. Application of the Kuramoto model and implementation of self-regulation after 500 time steps:
   (a) Recovery of previously deleted edges (if there are) with probability p_r.
   (b) Identification of edges connecting synchronized nodes within the switchers defined at the beginning of the simulation. These are the ones satisfying $\cos(\theta_i - \theta_j) > \sigma_{th}$, being θ_i and θ_j the phases of the connected nodes.
   (c) Deletion of the previously identified edges with a probability proportional to the Euclidean distance of the connected nodes.
4. Repetition of step 3 until the desired final time step is reached.

It is worth noting that the proportionality to the Euclidean distance mentioned at step 3.c has been considered since neuronal circuits tend to minimize wiring cost due to its important metabolic cost. Indeed, although long-distant connections exist, most links are short. [5]

This model offers a great number of possible study cases, as it has many parameters both in the system's definition (network and switchers) and in the dynamics, from the Kuramoto model parameters to the ones added in the self-regulation process, σ_{th} and p_r.

With the aim to identify the general traits of the behaviour of the system under that dynamics, we have analysed the response of the two network structures already presented (Fig. 1) setting two different synchronization thresholds, $\sigma_{th} = 0.7$ and 0.9. By analysing different values of σ_{th} we would be able to see the effects of considering damage on a more restricted selection of edges or on a wider assortment. In addition, we have also considered two options for the recovery of previously deleted edges, $p_r = 0.2$ and 0, to analyse the response of the system with and without the presence of recovery of the network structure. Therefore, the results presented in the next section show for, each network, the considered synchronization threshold and recovery probability.

It is worth noting that $g(\omega)$ has been defined as a Gaussian distribution with mean and variance equal to one, $\mathcal{N}(1, 1)$, in all the results presented in this work. In addition, the coupling strength has been set as $K = 2$, after verifying that this value is above the critical K_c in all cases, thus ensuring the spontaneous tendency to synchronization of the system when no self-regulation is applied.

IV. RESULTS

A. Local synchrony vs global synchrony

Bearing in mind the stochasticity of the process, all results presented in this section correspond to the average over 10 realizations to better notice the tendency of each case. It is important to mention that each realization starts with the definition of the network. Although each realization results from the same parameter configuration, the created networks have a different configuration. In other words, each realization shapes its unique network, switchers' location and initial conditions; but all of them are equivalent since they are defined with the same parameters.

1. 4 modules network

We have analysed the 4 modules network structure with the parameters specified in Fig. 1, (N, L, ρ, γ, n_c)=(60, 25, 6, 0.8, 24). In that case we have considered a total of 24 switchers of radius $R = 5$, which set an approximately 48% of the surface of the network covered by the switchers.

Firstly, let us take a look at the results with no recovery considered, $p_r = 0$ (Fig. 7, $\sigma_{th} = 0.7$; Fig. 8, $\sigma_{th} = 0.9$).

For both synchronization thresholds taken into account, we can see how both local and global order parameters split and decay separately.

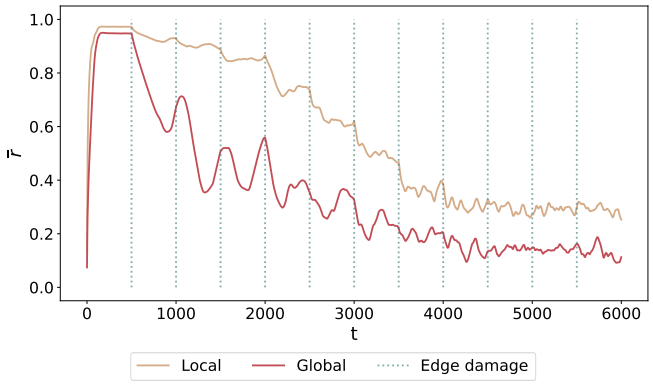

FIG. 7. Average evolution of the local and the global order parameters over 10 different realizations taking the 4 modules network structure and setting a low synchronization threshold, $\sigma_{th} = 0.7$, without considering the recovery of previously deleted edges, $p_r = 0$.

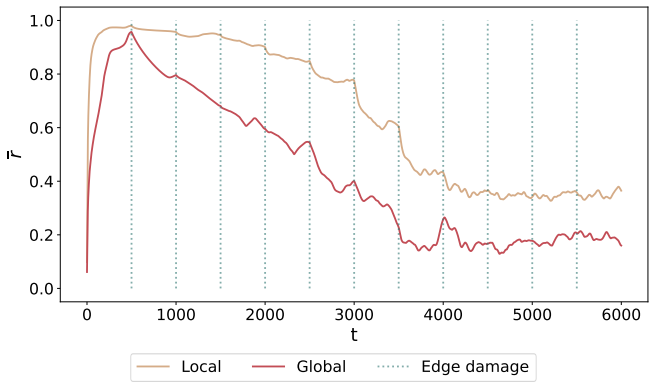

FIG. 8. Same case as figure 7, but setting a high synchronization threshold, $\sigma_{th} = 0.9$.

For all cases, the local order parameter is higher than the global one, which is completely expected since the connectivity within modules is stronger and more robust than when considering the network as a whole. Furthermore, intermodular edges are more vulnerable to damage due to the fact that they physically connect distant nodes. These two aspects are in accordance with the results, as they show how global synchronization is much more sensitive to damage.

Regarding the decay, we can appreciate it after each damage episode and we can see that it is slower and with smaller fluctuations for the more restrictive synchronization threshold, $\sigma_{th} = 0.9$, as expected. For a low value of σ_{th}, a more general damage is done to the system as highly synchronized nodes and not so synchronized ones are disconnected, which has an effect on the overall synchronization state of the system, here quantified with the global and local order parameters. However, for a highly restrictive threshold, all candidate edges to be deleted are highly synchronized, hence highly localized in the range of $\cos(\theta_i - \theta_j)$. This leads to a more controlled and less harmful damage to the system.

In addition, we can see how, at time step $t \sim 4000$, both order parameters fluctuate around a given stationary value. That is because there is no chance of recovery for the deleted nodes and all edges regulated by the switchers have already been deleted, meaning that there are no edges left to be removed. At this point, no structural damage is inflicted to the system and that is why the synchronization of the system does not change significantly. Nevertheless, even though no alteration on the network structure is taking place, there are tiny but still present fluctuations. It is because at this point the network is completely destroyed; it is not robust any more and the Kuramoto dynamics is remarkably sensitive to that aspect, overall resulting in an unstable evolution of the system.

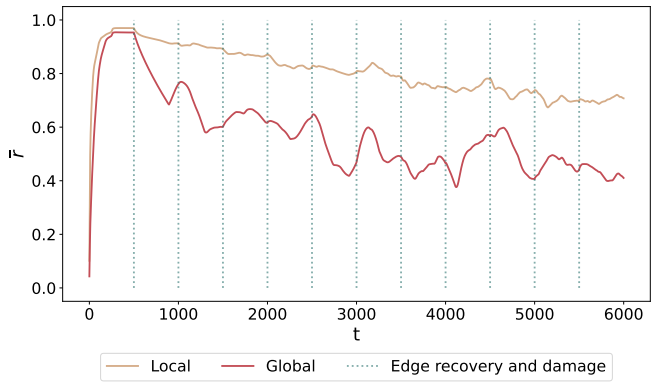

FIG. 9. Average evolution of the local and the global order parameters over 10 different realizations taking the 4 modules network structure and setting a low synchronization threshold, $\sigma_{th} = 0.7$, considering the recovery of previously deleted edges with a probability of $p_r = 0.2$.

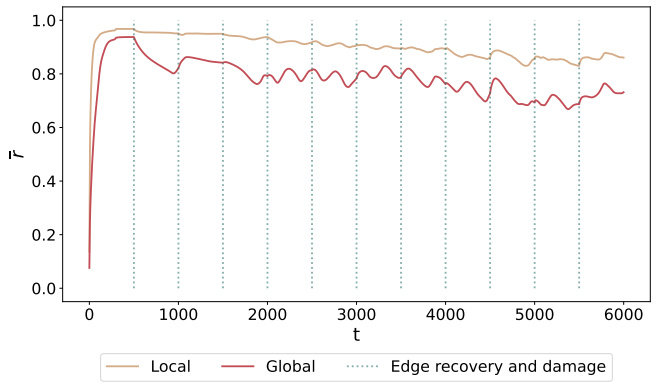

FIG. 10. Same case as figure 9, but setting a high synchronization threshold, $\sigma_{th} = 0.9$.

However, this dynamics is not realistic as it considers only damage and we are just destroying the system. In the next cases we have added the possibility of recovering prior deleted edges with probability $p_r = 0.2$, as shown in Fig. 9 for $\sigma_{th} = 0.7$, and in Fig. 10 for $\sigma_{th} = 0.9$.

Here we can also see how the local and the global order parameters split, but in contrast to the previous cases, the decay of both is much more slower due to the ability of deleted edges to recover. For $\sigma_{th} = 0.7$, we can see how the difference between both order parameters is higher than for $\sigma_{th} = 0.9$. That is because damage is done to highly and not so highly synchronized edges, making the system more vulnerable to each attack. That vulnerability can be seen in the decay of both parameters, which is faster than for $\sigma_{th} = 0.9$, where both keep quite more stable in time. It is also remarkable to say that for a more restrictive synchronization threshold, $\sigma_{th} = 0.9$, both the local and the global order parameters stay with high values in time, as expected.

2. *12 modules network*

Let us introduce the results of the 12 modules network structure built as explained in the previous sections, defining $(N,\ L,\ \rho,\ \gamma,\ n_c)$=(60, 25, 6, 0.8, 24). Here we have considered 72 switchers of radius $R = 5$, just to keep the same percentage of surface of the network covered by the switchers as in the last case, approximately 48%.

For this bigger and more complex structure than the last one, the obtained results turn out to be quite interesting. Following the same structure than the previous case, Fig. 11 and 12 correspond to the cases without edge recovery, $p_r = 0$, while Figs. 13 and 14 to the ones with recovery with probability $p_r = 0.2$, being the synchronization threshold $\sigma_{th} = 0.7$ and 0.9, respectively, for these cases.

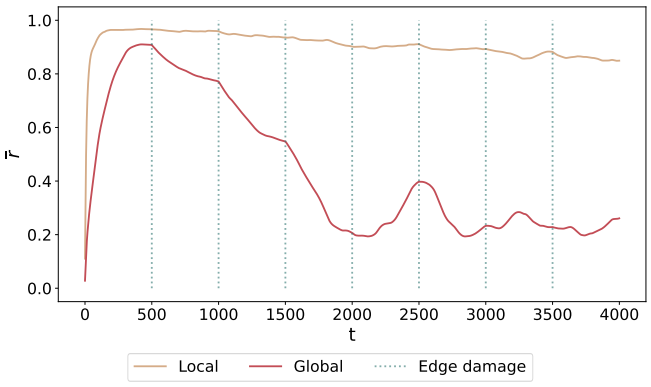

FIG. 11. Average evolution of the local and the global order parameters over 10 different realizations taking the 12 modules network structure and setting a low synchronization threshold, $\sigma_{th} = 0.7$, without considering the recovery of previously deleted edges, $p_r = 0$.

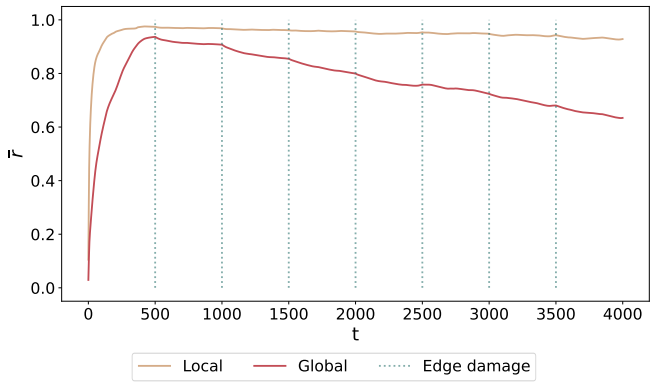

FIG. 12. Same case as figure 11, but setting a high synchronization threshold, $\sigma_{th} = 0.9$.

We observe that, on the one hand, in the case of $p_r = 0$ we can see how for both synchronization thresholds, the local order parameter stays high and outstandingly quite stable through time in spite of the lack of edge recovery, while the global one decays after each damage process (see Figs. 11 and 12). It is worth mentioning that the decay of the global order parameter is much more gradual for the $\sigma_{th} = 0.9$ case.

On the other hand, for the $p_r = 0.2$ case study we can appreciate that the local order parameter also stays high and stable through time, while the global one smoothly decays for $\sigma_{th} = 0.7$ and 0.9 (see Figs. 13 and 14).

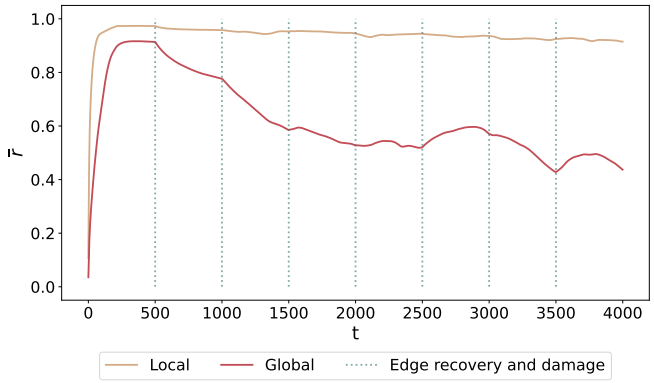

FIG. 13. Average evolution of the local and the global order parameters over 10 different realizations taking the 12 modules network structure and setting a low synchronization threshold, $\sigma_{th} = 0.7$, considering the recovery of previously deleted edges with a probability of $p_r = 0.2$.

If we compare the results of the 12 modules network with the ones of the 4 modules one, we can observe several differences. Firstly, in all cases for the 12 modules network, we obtain rather constant and high values for the local order parameter, even when $p_r = 0$ and damage recovery is not possible. This is probably due to the the much higher structural richness of the 12 modules network, enabling the system to be locally synchronized

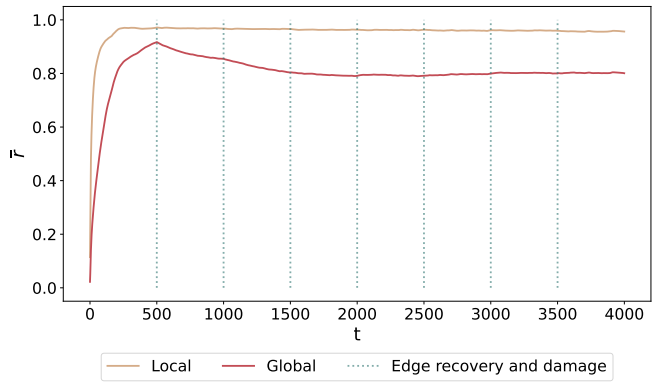

FIG. 14. Same case as figure 13, but setting a high synchronization threshold, $\sigma_{th} = 0.9$.

despite the presence of damage. Secondly, we can see in the 12 modules network how the difference between local and global order parameters ends up being larger in all cases, in spite of splitting at a slower pace in comparison to the 4 modules network. Thirdly, and lastly, it is worth saying that in the 12 modules, and in contrast to the smaller network, not so many fluctuations are observed (see Fig. 14 as a remarkable example). As a consequence, we believe that, in general, the structure of the network defining the system indubitably affects the response, and that the richness of the network eases the control of both local and global synchronization in a more robust way.

3. *Effect of modularity*

Another aspect we were interested in is the effect of modularity in network dynamics. Modularity is the responsible of local synchronization and, after the qualitative analysis performed in the previous sections, we wanted to analyse its effects in a quantitative manner.

To do it, we have studied the 4 modules network structure with the same parameters as before with the exception of the number of inter-modular connections, n_c. By doing so, the interaction between the modules becomes stronger, or not, depending on the value of n_c, which obviously has an strong effect on modularity.

According to [25], modularity is defined as

$$Q = \frac{1}{2m} \sum_{ij} \left(A_{ij} - \frac{k_i k_j}{2m} \right) \delta(c_i, c_j), \tag{7}$$

where m is the number of edges of the network, A is its adjacency matrix, k_i is the degree of node i and $\delta(c_i, c_j)$ is 1 if i and j belong to the same community and 0 if they do not.

The studied cases can be found in Table II, that perfectly shows how modularity is inversely proportional to the number of inter-modular connections.

For each network structure, we have quantified the effect of modularity by computing the relative difference between the integrals of the curves describing the temporal evolution of the local and the global order parameter. In other words, for each value of n_c we have computed the value of $\Delta A/A_0$ for several realizations, being ΔA and A_0 defined as

$$\Delta A = \int r_{local} dt - \int r_{global} dt, \tag{8}$$

$$A_0 = \int r_{local} dt. \tag{9}$$

The value of $\Delta A/A_0$ can be interpreted as the difference between both curves, as large values correspond to strong differences between local and global order parameters, meaning that the system is locally but not globally synchronized.

TABLE II. Number of inter-modular connections, n_c, and average modularity, $\overline{Q}$, over 100 networks of 4 modules created by setting (N, L, ρ, γ)=(60, 25, 6, 0.8) and the respective value of n_c.

n_c	$\overline{Q}$
6	0.745
12	0.725
24	0.685
36	0.652
48	0.616
60	0.583

It is worth noting that the dynamical model has been applied considering the case of having a recovery probability $p_r = 0.2$ and a synchronization threshold of $\sigma_{th} = 0.7$. In this context, our results show that $\Delta A/A_0$ grows exponentially with the modularity of the network defining the system, meaning that the switchers regulating the system are much more effective in highly modular systems (see Fig. 15). That is completely in agreement with the expected result, as highly modular systems have less inter-modular edges which, in turn, make the system more vulnerable to damage. With a lower number of inter-modular edges, the modules are less interconnected and it is easier to reach a greater local synchronization while having the whole system poorly synchronized.

B. Dynamic pattern formation

As modules interact with each other, it results appropriate to analyse the synchronization between them. To this end, we have identified each module with a label, as shown in Fig. 16, and we have computed the mean phase, $\overline{\theta}$, of each module at a certain time step. Then, we have computed $\cos(\overline{\theta}_i - \overline{\theta}_j)$ for all pairs of modules, what leads to an easy identification of which modules are synchronized, $\cos(\overline{\theta}_i - \overline{\theta}_j) \simeq 1$, and which do not and evolve independently, $\cos(\overline{\theta}_i - \overline{\theta}_j) \simeq 0$.

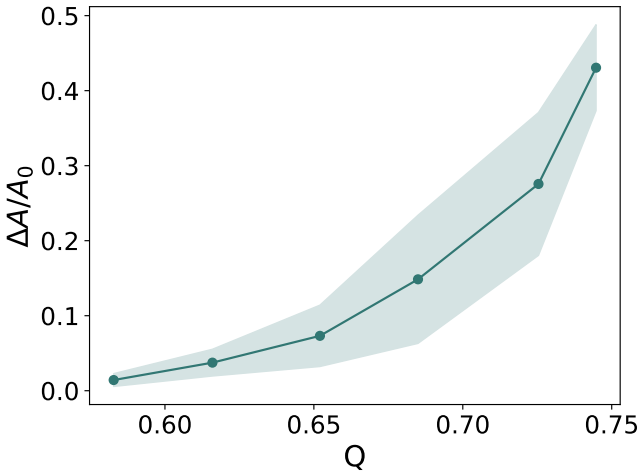

FIG. 15. Average value of the relative difference between the integrals of the temporal evolution of the local and the global order parameters, $\Delta A/A_0$, as a function of the modularity of the network analysed, Q. The averaging has been performed over 10 different realizations of each case and the dynamical model has been applied considering $p_r = 0.2$ and $\sigma_{th} = 0.7$.

The values of $\cos(\overline{\theta}_i - \overline{\theta}_j)$ can be plotted as a matrix, where i corresponds to the row and j to the column. In order to detect patterns within the system, one can rearrange rows and columns accordingly to group the elements showing a greater correlation. An example illustrating an already rearranged $\cos(\overline{\theta}_i - \overline{\theta}_j)$ matrix can be found in Fig. 17, which perfectly shows three well-defined communities of highly synchronized modules at a particular instant of the simulation.

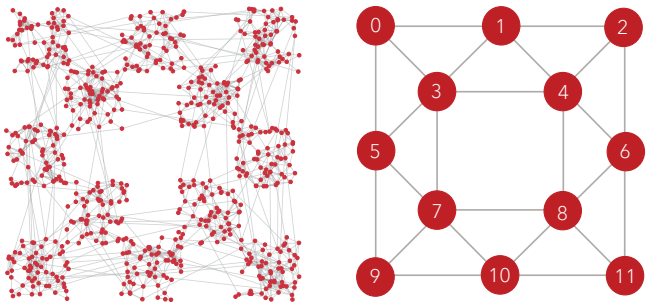

FIG. 16. Diagram showing the labels that identify the modules forming the 12 modules network.

If we keep the state of the system at different time steps, we can compute $\cos(\overline{\theta}_i - \overline{\theta}_j)$ for each kept instant and analyse if there is a recurrent structure in synchronization patterns through time.

With the purpose of detecting some kind of pattern in the correlation between modules, we have plotted the $\cos(\overline{\theta}_i - \overline{\theta}_j)$ matrices of the different selected instants with two different arrangement of rows and columns. Firstly, we have plotted each matrix according to its particular arrangement, leading to the best possible representation

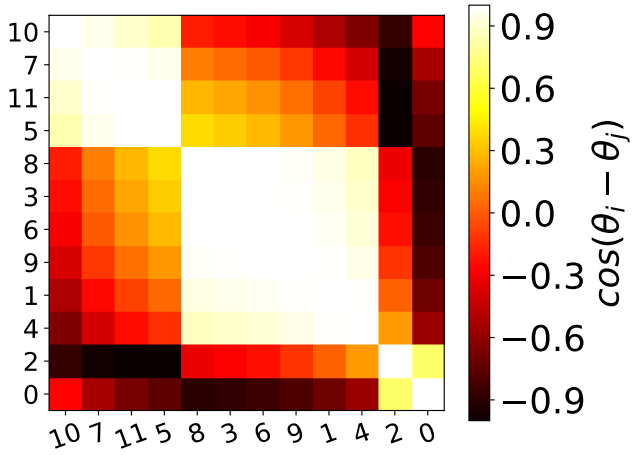

FIG. 17. Rearranged $\cos(\overline{\theta}_i - \overline{\theta}_j)$ matrix resulting from a simulation considering a 12 modules network, 72 switchers of $R = 5$, $K = 2$, $\sigma_{th} = 0.7$ and p_r=0.2, taking the state of the system at time step $t = 500$.

of the communities formed by highly synchronized modules. Secondly, we have plotted the matrices not with its particular best arrangement but with the one for the first instant, i.e. at the state of higher global synchronization. By comparing both plots, it is easy to see whether the interaction between modules follows a constant pattern or a time evolving one. Indeed, we can appreciate whether the pattern is the same or not. If that is the case, we can inspect whether the relationship between interacting modules remains constant or evolves through time.

The results are provided in Fig. 18, where the results from a single realization of the model are shown. The figure corresponds to a case taking the 12 modules network structure, 72 switchers of $R = 5$ and the dynamic parameters set as $(K, \sigma_{th}, p_r) = (2, 0.7, 0.2)$. As it can be seen, both local and global order parameters fluctuate substantially, which is due to the fact that only one realization is considered (in contrast to the previous cases, where the mean values over several realizations were represented). However, we can see the kind of behaviour seen in the previous case: the global order parameter substantially decays while the local one keeps high and stable over time. Edge recovery and damage has been performed as in all cases, every 500 time steps, and we have analysed the synchronization between modules at time steps $t = 500, 2000$ and 3500.

The $\cos(\overline{\theta}_i - \overline{\theta}_j)$ matrices of Fig. 18 show how there is an underlying structure in the synchronization between modules at different time steps. We can see how the first arrangement is completely lost as time goes by, but certain interactions are robust and persevere (see panels $a.1$, $b.2$ and $c.2$). However, new correlations emerge, evolving from a well-defined three communities setting ($a.1$) to a more diverse configuration ($c.1$). To sum up, there is a kind of dynamic pattern formation where correlations

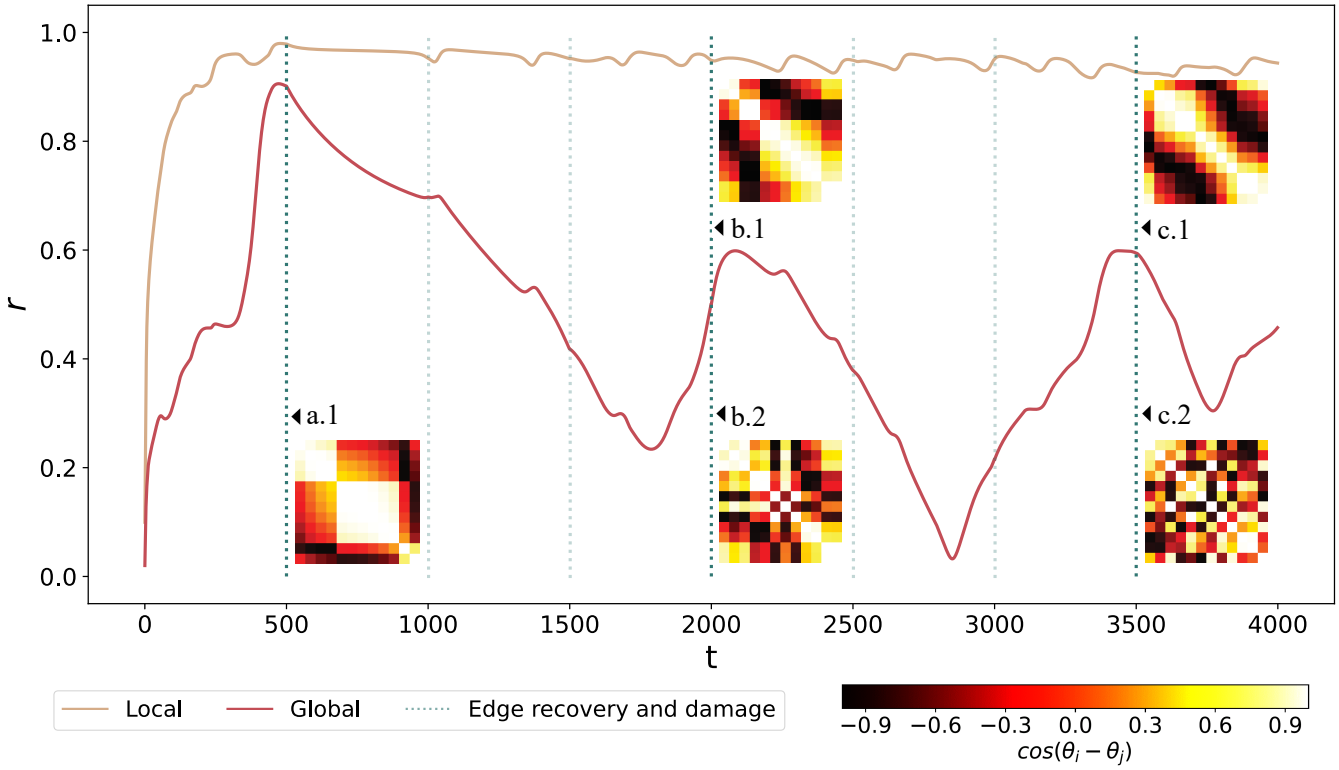

FIG. 18. Time evolution of the global and the local order parameters of a single realization of the model taking the 12 modules network, 72 switchers of $R = 5$ and setting $K = 2$, $\sigma_{th} = 0.7$ and p_r=0.2. The plot includes $\cos(\overline{\theta}_i - \overline{\theta}_j)$ matrices at $t = 500$ (case a), $t = 2000$ (case b) and $t = 3500$ (case c). For case a, only the plot with the best arrangement for detecting the present communities is shown (a.1). For cases b and c we also show the plots of the matrices conveniently rearranged for each case (b.1 and c.1), but we also include the same matrices rearranged following the same rows and columns order than a.1 (figs. b.2 and c.2).

between modules change in time but some interactions persist, which gives rise to the presence of an underlying structure.

V. DISCUSSION AND CONCLUSIONS

In silico modelling allows us to test whether a simplification of the currently known behaviour is sufficient to reproduce what we see in real neuronal cultures. Taking as inspiration the regulatory behaviour of glial cells in neuronal networks, we have modelled a self-regulation dynamics on a network of Kuramoto oscillators. The basis of our model consists in damaging edges connecting highly synchronized nodes with the possibility of recovering them after a certain period of time. Several conclusions can be drawn from our study.

Firstly, we have seen how localized self-regulation makes possible to attain high local synchronization and low global one, despite acting on a system that spontaneously tends towards synchronization. In real neuronal networks, glial cells act within their domain. Favoring local synchronization while keeping low global synchronization is a kind of state that is considered to correspond to a well-functioning neuronal system. In conclusion, the results obtained are absolutely satisfactory as it means that, despite the simplicity of our model, it is sufficient to control synchronization at different scales and consequently to reproduce traits observed in nature.

Secondly, we have analysed the effects of the multiple parameters of the model. Regarding the size of the switchers' domain, we have seen how smaller switchers but greater in number are much more efficient that less but large ones, in spite of covering the same surface. The nature of that feature is completely geometrical, but it is important to bear it in mind when defining the switchers regulating the system. In reference to the synchronization threshold, σ_{th}, it has been noticed that the decay of both global and local order parameters is slower and that the difference between both order parameters is smaller when it is more restrictive, as expected. Concerning the recovery probability for previously deleted edges, we spotted that it enables the reach of a quite stationary behaviour of both order parameters when it is not zero, as it prevents the system from getting completely damaged.

Thirdly, we have analysed the effects of modularity. Neuronal cultures and the brain itself are characterized

by their modularity and, as a consequence, the consideration of modular networks in that project turns out to be appropriate. However, it has been interesting to see how, indeed, modularity promotes the reach of local synchronization with global disorder.

Last but not least, it is proven that a larger and therefore more complex network leads to richer results. Our results show how complex networks give rise to high and stable local synchronization and simultaneous global disorder in the presence of self-regulation in all studied cases. This result is highly relevant as this behaviour is the one seen in nature and here we see how complexity eases it. In addition, the richness of this kind of dynamics on complex networks goes further. We have discovered a dynamic pattern formation when analysing the synchronization between pairs of modules and their evolution. There is a pattern formed by groups of modules highly synchronized that evolves in time. Each instant has a different one, but there is an underlying structure as some interactions remain robust.

This work started with a very simple proposal. The model is a simplification of the highly complex and still not fully known dynamical problem such as the brain self-regulation. Nevertheless, our results show that it is enough to obtain the overall behaviour we were interested in: local synchronization without global one only throughout localized actions over the system. That is what makes the model useful and powerful, as it is simple but sufficient. Through the realization of the project we have found answers, but we have also come up with new questions. Does the dynamic pattern formation detected follow any kind of periodic behaviour? And if it does, is it robust to perturbations? How would the robustness of this dynamics be with respect to the addition of noise? In neuroscience it is really common to work with weighted networks and inhibitory as well as excitatory interactions. Here we opted for a simple and general representation of the system, but the consideration of those aspects would be interesting to see the degree of affectation of them to the resulting behaviour of the system.

These open questions mentioned above give rise to new directions and it is relevant to keep in mind that self-regulation in networks showing synchrony at any level can be seen in other systems beyond neuroscience. For this reason, we believe that our model can be generally applied to investigate the effects of self-regulation in other kind of temporally correlated systems, such as social or transportation networks.

ACKNOWLEDGMENTS

I would like to express my deepest gratitude to Albert Díaz-Guilera and Jordi Soriano for their guidance, advice and patience throughout these months. I also thank Albert for introducing me to the wonderful world of complex systems years ago and for encouraging me to follow this path; and Jordi for his endless enthusiasm and for introducing me to the beautiful field of neuroscience.

I would also like to thank Irene Ferri for her help and advice, my friends for their support, and specially my parents, for their unconditional love.

[1] S. H. Strogatz, *Sync: how order emerges from chaos in the universe, nature, and daily life*, 1st. ed. New York, NY, USA: Hyperion, 2003.

[2] S. Chakravartula, P. Indic, B. Sundaram and T. Killingback, "Emergence of local synchronization in neuronal networks with adaptive couplings". *PLoS ONE*, vol. 12, no. 6, e0178975, 2017.

[3] S. Kazemi and Y. Jamali, "Phase synchronization and measure of criticality in a network of neural mass models". *Sci Rep* 12, 1319, 2022.

[4] P. Uhlhaas, G. Pipa, B. Lima, L. Melloni, S. Neuenschwander, D. Nikolić, et al. "Neural synchrony in cortical networks: history, concept and current status". *Front Integr Neurosci.*, vol. 3, 2009.

[5] A. Arenas, A. Díaz-Guilera, J. Kurths, Y. Moreno and C. Zhou, "Synchronization in complex networks", *Physics Reports*, vol. 469, no. 3, pp. 93-153, 2008.

[6] J. Fell and N. Axmacher, "The role of phase synchronization in memory processes." *Nat Rev Neurosci*, vol. 12, pp. 105–118, 2011.

[7] A. K. Kreiter, and W. Singer, "Stimulus-dependent synchronization of neuronal responses in the visual cortex of the awake macaque monkey." *J Neurosci.*, vol. 16, no. 7, 2381–2396, 1996.

[8] A. Araque, M. Navarrete, "Glial cells in neuronal network function". *Philos Trans R Soc Lond B Biol Sci.* 365(1551), 2375-2381, 2010.

[9] S. Makovkin, E. Kozinov, M. Ivanchenko, et al. "Controlling synchronization of gamma oscillations by astrocytic modulation in a model hippocampal neural network". *Sci Rep*, vol. 12, 6970, 2022.

[10] D. C. Patel, B. P.Tewari, L. Chaunsali, H. Sontheimer, "Neuron-glia interactions in the pathophysiology of epilepsy." *Nat Rev Neurosci.* vol. vol. 20, no. 5, pp. 282-297, 2019.

[11] G. Carola, D. Malagarriga, C. Calatayud, et al. "Parkinson's disease patient-specific neuronal networks carrying the LRRK2 G2019S mutation unveil early functional alterations that predate neurodegeneration." *npj Parkinsons Dis.* vol. 7, no. 55, 2021.

[12] T. Menara, G. Baggio, D. Bassett, et al. "Functional control of oscillator networks". *Nat Commun*, vol. 13, no. 4721, 2022.

[13] L. Papadopoulos, J. Z. Kim, J. Kurths, and D. S. Bassett, "Development of structural correlations and synchronization from adaptive rewiring in networks of Kuramoto oscillators." *Chaos: Interdiscip. J. Nonlinear Sci.*, vol. 27, no. 073115, 2017.

[14] M. Fazlyab, F. Dörfler and V. M. Preciado, "Optimal network design for synchronization of coupled oscillators." *Automatica*, vol. 84, pp. 181–189, 2017.

[15] A. Forrow, F. G. Woodhouse and J. Dunkel, "Functional control of network dynamics using designed Laplacian spectra." *Phys. Rev. X*, vol. 8, no. 041043, 2018.

[16] E. Bullmore and O. Sporns, "Complex brain networks: graph theoretical analysis of structural and functional systems.", *Nat. Rev. Neurosci.*, vol. 10, pp. 186–198, 2009.

[17] V. Braitenberg and A. Schüz *Statistics and Geometry of Neuronal Connectivity*, Springer, Berlin, 1998.

[18] D. Meunier, R. Lambiotte, A. Fornito, et al. "Hierarchical modularity in human brain functional networks", *Front. Neuroinform.*, vol. 3, 2009.

[19] H. Yamamoto et al. "Impact of modular organization on dynamical richness in cortical networks." *Sci. Adv.*, vol. 4, no. 11, pp. eaau4914, 2018.

[20] Y. L. Maistrenko, B. Lysyansky, C. Hauptmann, O. Burylko, and P. A. Tass, "Multistability in the Kuramoto model with synaptic plasticity." *Physical Review E*, vol. 75, no. 6, 2007.

[21] D. Hansel, G. Mato, and C. Meunier, "Phase dynamics for weakly coupled Hodgkin-Huxley neurons" *Europhys. Lett*, vol. 23, no. 5, pp. 367-372, 1993.

[22] Y. Kuramoto, "Self-entrainment of a population of coupled non-linear oscillators." In: Araki, H. (eds) *International Symposium on Mathematical Problems in Theoretical Physics. Lecture Notes in Physics*, vol. 39, Springer, Berlin, 1975.

[23] X. Li, "The role of degree-weighted couplings in the synchronous onset of Kuramoto oscillator networks." *Physica A: Statistical Mechanics and its Applications*, vol. 387, Issue 26, pp. 6624-6630, 2008.

[24] T. Ichinomiya, "Frequency synchronization in a random oscillator network." *Physical review. E, Statistical, nonlinear, and soft matter physics*, vol. 70 2 Pt 2, Art. no. 026116, 2004.

[25] M. E. J. Newman, *Networks: An Introduction*, p. 224. Oxford University Press, 2011.

[26] J. Reichardt and S. Bornholdt, "Statistical Mechanics of Community Detection," *Phys. Rev.* E 74, 016110, 2006.